IOP Conf. Series: Materials Science and Engineering **369** (2018) 012022 doi:10.1088/1757-899X/369/1/012022

Microstructure and critical strain of dynamic recrystallization of 6082 aluminum alloy in thermal deformation

W W Ren[1,2], C G Xu[1], X L Chen[1] and S X Qin[1]

[1]Beijing Research Institute of Mechanical and Electrical Technology, Beijing 100083, China

E-mail: renweiwei2009@126.com

Abstract. Using high temperature compression experiments, true stress true strain curve of 6082 aluminium alloy were obtained at the temperature 460℃-560℃ and the strain rate 0.01 s^{-1}-10 s^{-1}. The effects of deformation temperature and strain rate on the microstructure are investigated; $(-\partial \ln\theta / \partial\varepsilon) - \varepsilon$ curves are plotted based on σ-ε curve. Critical strains of dynamic recrystallization of 6082 aluminium alloy model were obtained. The results showed lower strain rates were beneficial to increase the volume fraction of recrystallization, the average recrystallized grain size was coarse; High strain rates are beneficial to refine average grain size, the volume fraction of dynamic recrystallized grain is less than that by using low strain rates. High temperature reduced the dislocation density and provided less driving force for recrystallization so that coarse grains remained. Dynamic recrystallization critical strain model and thermal experiment results can effectively predict recrystallization critical point of 6082 aluminium alloy during thermal deformation.

1. Introduction

Dynamic recrystallization (DRX) plays an important role in controlling grain size during metal thermal forming. It not only can refine grains, but also control mechanical properties and electrical properties [1,2]. It is now recognized as a powerful tool to control the structure and properties of metals under industrial processing operations [3]. True stress and true strain can be obtained by Gleeble thermal simulation experiment under constant temperature and strain rates. Microstructure and grain size after dynamic recrystallization can be investigated by EBSD. Study of the relationship between the deformation parameters and the microstructure evolution is of great significance for controlling the properties of the material [4].

Deformation temperature and strain rate are two important deformation parameters of materials. The relationship between flow stress and strain is established through $\sigma - \varepsilon$ curve [5]. The occurrence of DRX is indicated by the appearance of a peak in the stress –strain curve. However, DRX is actually initiated before the strain corresponding to the peak stress. This threshold strain is known as the critical strain [6,7]. The difficulty is how to measure the critical strain, where the material begins to recrystallize dynamically. Jonas pointed out that the hardening rate(θ)-stress(σ) curve can be obtained by processing the $\sigma - \varepsilon$ curve. The inflection point of $\theta - \sigma$ curve is the critical stress, the corresponding strain of which is critical strain ε_c. Poliak E I *et al* [8] study shows that the relationship between the hardening rate and the stress is equivalent to the relationship between the logarithm of the hardening rate and the strain. Guo H L *et al* [9] obtained the critical strain model of the dynamic recrystallization of 7075 aluminum alloy through the compression test and simulated

the dynamic recrystallization process by Finite Element Method (FEM), the result show the model was verified; Chen X H *et al* [10] studied the effect of temperature and strain rates on microstructure of 7085 aluminum alloy in high temperature and investigated the critical strain model; Shi L *et al* [11] researched on critical strain model and results indicate model is in good agreement with the experiment. The dynamic recrystallization behavior of various aluminum alloy materials has been studied widely. At present there are few studies on the dynamic recrystallization of 6082 aluminum alloy.

The stress-strain curves were obtained alloy based on thermal compression experiment of the 6082 aluminum alloy, $(-\partial \ln\theta / \partial\varepsilon) - \varepsilon$ curve are 2 order polynomial fitted at different temperatures and strain rates, the extremum point of the curve is critical strain of the dynamic recrystallization. According to the experimental data of EBSD grain, recrystallized grain evolution and dynamic recrystallization fraction distribution is researched. The process of dynamic recrystallization can be simulated by FEM base on the experimental data which will be helpful to better control the internal microstructure and mechanical properties of the 6082 aluminum alloy.

2. Experimental procedure

The chemical composition(wt.%) of 6082 aluminum alloy is 0.93 Si, 0.165 Fe, 0.056 Cu, 0.454 Mn,0.65 Mg, 0.117 Cr, 0.002 Zn, 0.03 Ti, The initial average grain size is 60 μm. The specification of raw materials is Φ30 mm×1000 mm, compressed specimens are machined to dimension Φ10 mm×15 mm, both the surface are perpendicular to the axis, the axis is parallel to the compression direction. The forming temperature is 460℃, 500℃, 540℃, 560℃ and the strain rate is 0.01 s^{-1}, 0.1 s^{-1}, 1 s^{-1}, 10 s^{-1}. The operation model of the thermal simulator is Gleeble-3500,heating speed of 1℃. s^{-1}, the specimens are heat preserved for three minutes when up to the set temperature. After the compression is finished, specimens are immediately quenched in water to retain the deformed microstructure. The compressed specimens are sectioned along the axial direction, microstructure is characterized by electro-polishing of the specimens for 10 seconds with voltage 20 V and current 1 A in a solution consisting of 10% perchloric acid and 90% ethanol. By EBSD observation of the internal microstructure, it is grain disorientation greater than or equal to 10° that distinguish the grain boundaries. On account of detection limitation in microstructure [12], the grain misorientation less than 3 degrees is not considered.

3. Results and discussions

3.1. Stress-strain curves

The true stress-true strain curves of 6082 aluminum alloy deformed at different temperatures and strain rates are shown in figure 1. It is seen that the flow stress is increased with increasing strain rate and decreasing temperature. When the strain rates are 0.01 s^{-1} and 0.1 s^{-1}, all the flow curves exhibit a peak and then follow by gradual fall to a steady stress state which is indicative of the occurrence of DRX [13]. In the steady state, the hardening and the softening due to DRX are in a state of balance, flow stress almost remain the same with the increase of deformation. When the strain rates are 1 s^{-1} and 10 s^{-1}, stress-strain curves are in fluctuation. Stress peaks and troughs appears alternately, which shows that the working hardening and the dynamic recrystallization played the dominant role alternately.

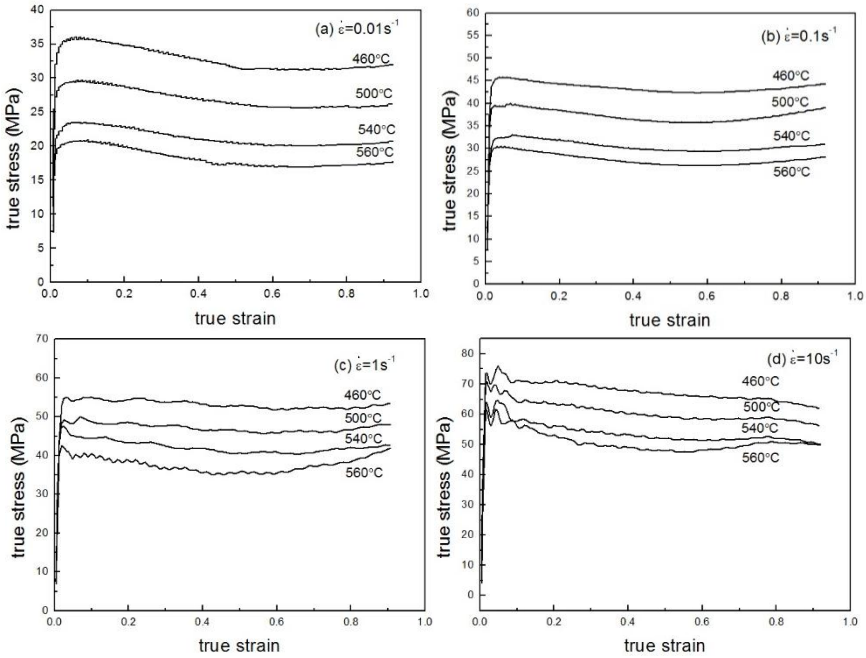

Figure 1. True stress-strain curves of 6082 Al-Si-Mg aluminum alloy at different strain rates o(a)$\dot{\varepsilon} = 0.01$ s^{-1} (b) $\dot{\varepsilon} = 0.1$ s^{-1} (c) $\dot{\varepsilon} = 1$ s^{-1} (d) $\dot{\varepsilon} = 10$ s^{-1}.

3.2. Stress-strain constitutive equations

Arrhenius equation describes the hot deformation behavior of mental [14], and gives equation between Zener−Holloman parameter and flow stress σ. This theory can be expressed as in equations (1)-(3):

$$Z = \dot{\varepsilon} \mathrm{e}^{Q/(RT)} \tag{1}$$

$$\dot{\varepsilon} = AF(\sigma)\mathrm{e}^{Q/(RT)} \tag{2}$$

$$F(\sigma) = \begin{cases} \sigma^{n_1}, \alpha\sigma < 0.8 \\ \mathrm{e}^{\beta\sigma}, \alpha\sigma > 1.2 \\ [\sinh(\alpha\sigma)]^n, \text{for all } \sigma \end{cases} \tag{3}$$

σ is flow stress (MPa); Q is activation energy (kJ mol^{-1}); $\dot{\varepsilon}$ is strain rate (s^{-1}) ;T is temperature (K); R is constant (8.314 J (mol K)$^{-1}$); α, β and n_1 are material constants , $\alpha=\beta/n_1$.

Based on the figures 2(a) and 2(b), the values β and n_1 are evaluated, β and n_1 are the average value of the slopes of the $\ln\dot{\varepsilon} - \sigma$ curve and $\ln\dot{\varepsilon} - \ln\sigma$ curve.

Activation Q can be calculated as follows:

$$Q = R\left(\frac{\partial \ln\dot{\varepsilon}}{\partial \ln[\sin(\alpha\sigma)]}\right)_T \left[\frac{\partial \ln[\sinh(\alpha\sigma)]}{\partial(1/T)}\right]_{\dot{\varepsilon}} \tag{4}$$

The figures 2(c) and 2(d) illustrates the relationships among $\ln\dot{\varepsilon}$, $\ln[\sin(\alpha\sigma)]$ and T^{-1}.

According to the above equation and figure 2, the material constants are listed in table 1.

Table 1. Material constants of Al-Si-Mg alloy.

$\alpha(\mathrm{MPa}^{-1})$	n	$A(s^{-1})$	$Q(\mathrm{kJ \cdot mol}^{-1})$
0.0269	5.89	4.36×10^{10}	174.9

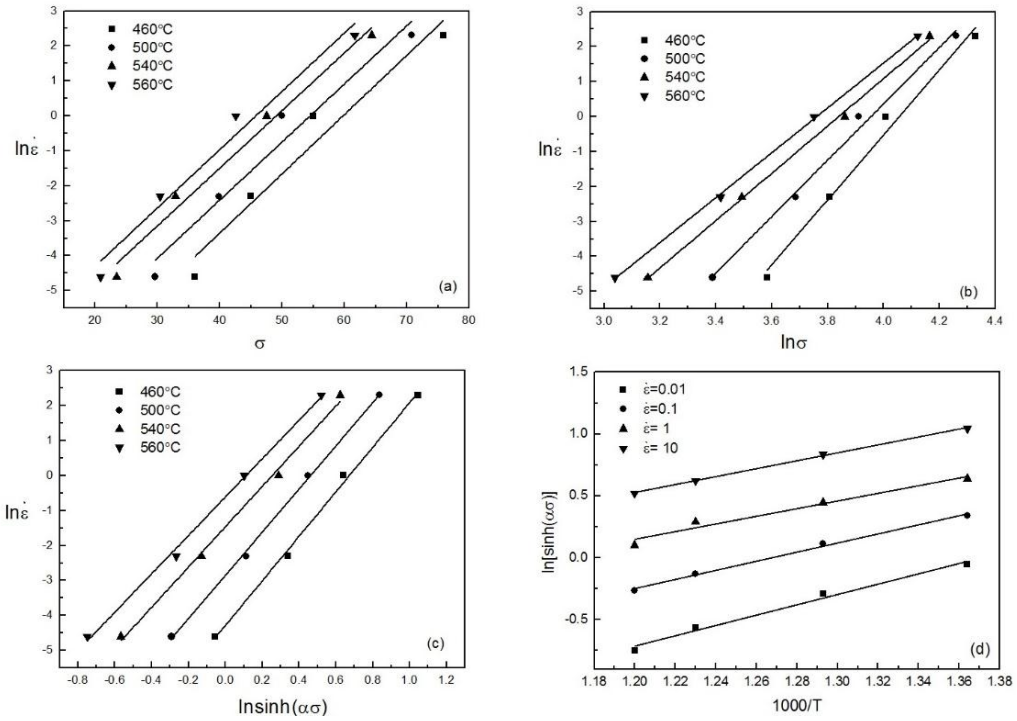

Figure 2. Linear relationships of various parameters of 6082 aluminum alloy: (a) $\ln\dot{\varepsilon} - \sigma$; (b) $\ln\dot{\varepsilon} - \ln\sigma$; (c) $\ln\dot{\varepsilon} - \ln\sinh(\alpha\sigma)$; (d)$\ln\sinh(\alpha\sigma) - T^{-1}$.

So the mathematic model for stress of 6082 Al-Si-Mg alloy is summarized as follows:

$$\sigma = 37.2\ln\left\{\left(\frac{Z}{4.36\times10^{10}}\right)^{\frac{1}{5.89}} + \left[\left(\frac{Z}{4.36\times10^{10}}\right)^{\frac{2}{5.89}} + 1\right]^{\frac{1}{2}}\right\} \tag{5}$$

$$Z = \dot{\varepsilon}e^{\frac{174.9}{8.31T}} \tag{6}$$

3.3. Effect of deformation parameters on microstructure

The figure 3 is EBSD image of grain structure when the temperature 540℃, true strain 0.6 and the strain rate 0.01s^{-1}, 0.1s^{-1}, 1s^{-1}, 10s^{-1}, Corresponding parameters ln*Z* is 21.3, 23.6, 25.9 and 28.2.

Red line is grain boundary. Dynamic recrystallization occurs at temperature 540℃ and different strain rates from photographs, average grain size of recrystallized grains decreases with the increase of strain rate. It is also conducted that the gains are relatively small under the conditions of high *Z*.

The figure 4 is EBSD image of recrystallization volume fraction when the temperature 540℃, true strain 0.6 and the strain rate 0.01 s^{-1}, 0.1 s^{-1}, 1 s^{-1}, 10 s^{-1}, blue represents dynamic recrystallization region, yellow is the not recrystallization region. Based on the data from EBSD post-processing software, the recrystallization volume fraction in (a) (b) (c) (d) are 78%, 60.3%, 67.8%, 69%. At lower strain rate, the dynamic recrystallization process is adequate, and the recrystallized grains have enough time to grow up (figures 4(a) and 4(b)). The dynamic recrystallization of materials is closely related to the deformation time, and the deformation time at high strain rate is short, and the dynamic recrystallization will be limited. The recrystallization volume fraction is decreased with the increase of strain rates or ln*Z*.

The results from grain evaluation and recrystallization volume fraction evaluation reveals that high strain rates will refine grains and low strain rates is beneficial to improve the fraction of dynamic recrystallization when temperature keep the same.

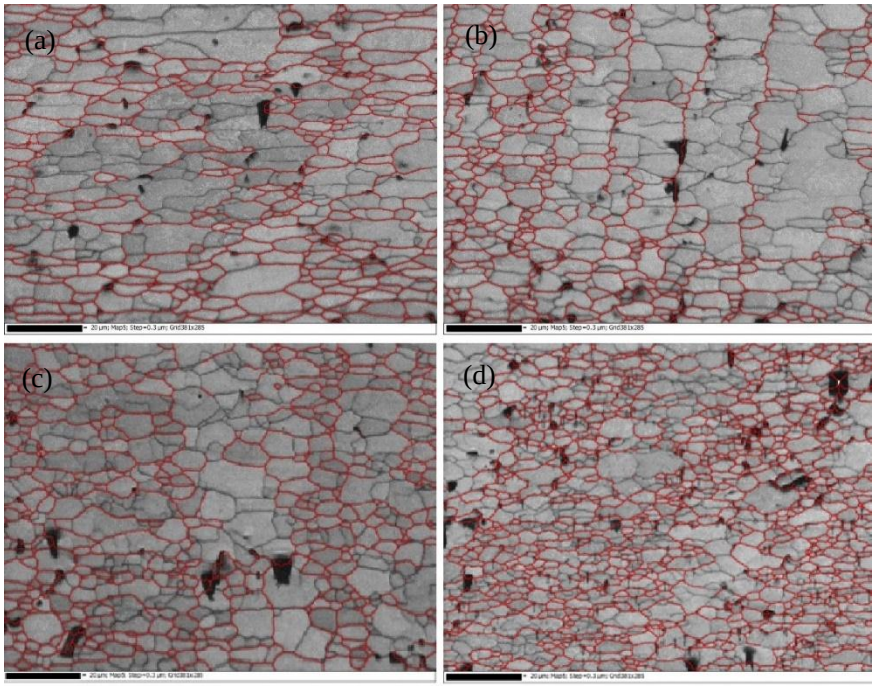

Figure 3. EBSD grain structure of 6082 aluminum alloy at different strain rates: (a) $\dot{\varepsilon} = 0.01\ s^{-1}$(ln$Z$=21.3); (b) $\dot{\varepsilon} = 0.1\ s^{-1}$(ln$Z$=23.6); (c) $\dot{\varepsilon} = 1\ s^{-1}$(ln$Z$=25.9); (d) $\dot{\varepsilon} = 10 s^{-1}$(ln$Z$=28.2).

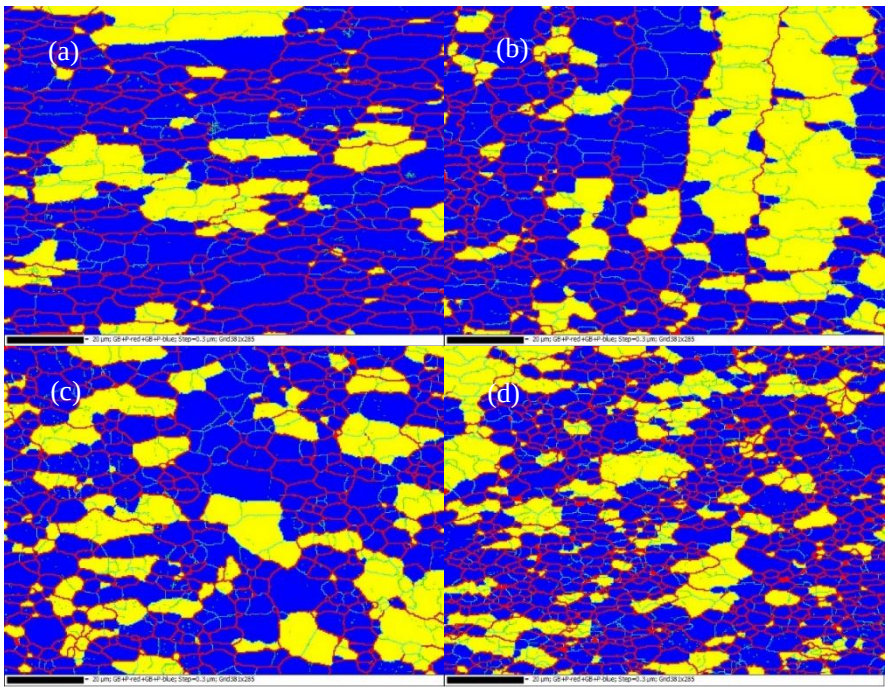

Figure 4. Recrystallization volume fraction of 6082 aluminum alloy at different strain rates: (a) $\dot{\varepsilon} = 0.01\ s^{-1}$ (ln$Z$=21.3); (b) $\dot{\varepsilon} = 0.1 s^{-1}$ (ln$Z$=23.6); (c) $\dot{\varepsilon} = 1\ s^{-1}$ (ln$Z$=25.9); (d) $\dot{\varepsilon} = 10\ s^{-1}$ (ln$Z$=28.2).

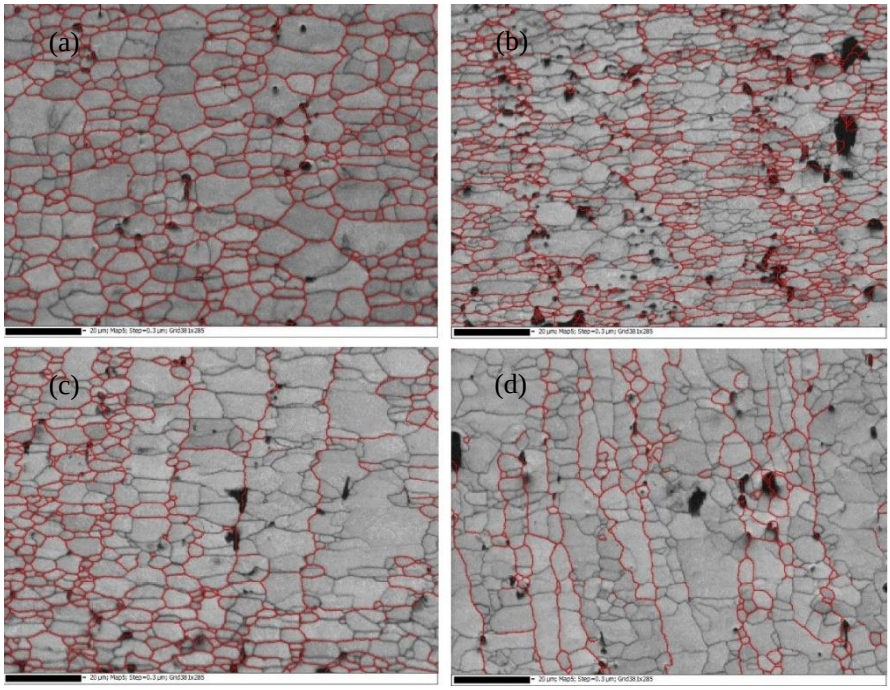

Figure 5. EBSD grain structure of 6082 aluminum alloy at different temperatures: (a) 460℃(lnZ=26.4); (b) 500℃ (lnZ=25); (c) 540℃ (lnZ=23.6); (d)560℃ (lnZ=23).

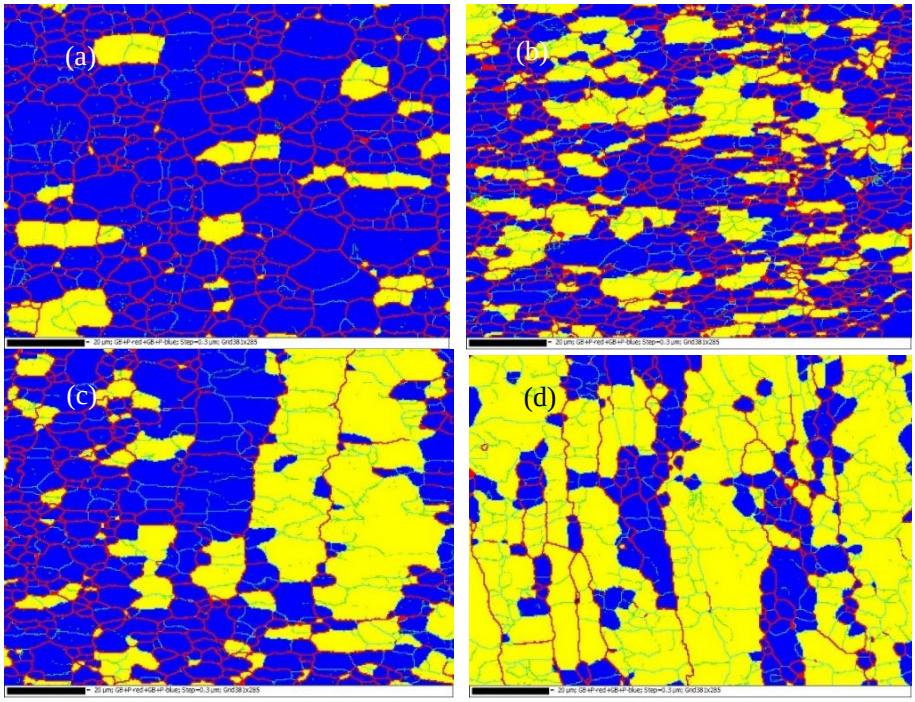

Figure 6. Recrystallization volume fraction of 6082 aluminum alloy at different strain rates: (a) 460℃ (lnZ=26.4); (b) 500℃ (lnZ=25); (c) 540℃ (lnZ=23.6); (d) 560℃ (lnZ=23).

The figure 5 is EBSD image of grain structure when the strain rate is 0.1 s^{-1}, true strain 0.6 and the temperature is 460℃, 500℃, 540℃, 560℃, Corresponding parameters ln$Z$ is 26.4, 25, 23.6 and 23. Red line is grain boundary. Dynamic recrystallization occurs at strain rate 0.1 s^{-1} and different temperatures from photographs. At lower temperatures recrystallization grains are equiaxed grains (figures 5(a) and 5(b)), which gradually transform to columnar grains as the equiaxed grains grow up to annex the small grains (figures 5(c) and 5(d)). Average grain size of recrystallized grains increases with the increase of deforming temperature.

With the increase of deforming temperature, the growth of recrystallized grain boundary enhanced. High temperature reduces dislocation density and provides a less driving force for dynamic recrystallization nucleation. As is shown in figure 6(d), blue represents dynamic recrystallization region.

From the figure 6 above, the deformation keeps similar, amount of recrystallization volume fraction increase as deformation temperature decrease at a given strain rate. The higher the deformation temperature, the smaller recrystallization volume fraction of the dynamic recrystallization. It is also shown that the dynamic recrystallization fraction decrease with the decrease of ln$Z$.

3.4. Critical strain of dynamic recrystallization

By experiment, the true stress-true strain curve is established, but it is difficult to reflect which strain the dynamic recrystallization is initiated from the curve [15]. Based on the Jonas critical strain theory, the critical strain ε_c is acquired as the follow equation [8]:

$$\frac{\partial}{\partial\sigma}\left(\frac{\partial\theta}{\partial\sigma}\right)_{\dot{\varepsilon}} = \frac{\partial}{\partial\varepsilon}\left(\frac{\partial\ln\theta}{\partial\varepsilon}\right)_{\dot{\varepsilon}} = 0 \tag{7}$$

$$\theta = \frac{\partial\sigma}{\partial\varepsilon} \tag{8}$$

Figure 7 shows the relationship between $(-\partial\ln\theta/\partial\varepsilon) - \varepsilon$ curves when the strain rate is 0.01 s^{-1} and true strain is 0.6 at different temperatures. By two order Polynomial fitting, the relationships between $(-\partial\ln\theta/\partial\varepsilon)$ and ε are listed at different temperatures and strain rates in table 2.

Table 2. Relationships between $-\partial\ln\theta/\partial\varepsilon$ and ε at different strain rates and temperatures.

$\dot{\varepsilon}$ (s^{-1})	T (℃)	$-\partial\ln\theta/\partial\varepsilon$-$\varepsilon$ relation
0.01	460	$-\partial\ln\theta/\partial\varepsilon = 251.29 - 9311.04\varepsilon + 129492.7\varepsilon^2$
	500	$-\partial\ln\theta/\partial\varepsilon = 290.24 - 9332.84\varepsilon + 104531.8\varepsilon^2$
	540	$-\partial\ln\theta/\partial\varepsilon = 206.30 - 4201.6\varepsilon + 47829.8\varepsilon^2$
	560	$-\partial\ln\theta/\partial\varepsilon = 286.35 - 6754.54\varepsilon + 95838.4\varepsilon^2$
0.1	460	$-\partial\ln\theta/\partial\varepsilon = 481.5 - 17012.1\varepsilon + 237154.1\varepsilon^2$
	500	$-\partial\ln\theta/\partial\varepsilon = 368.2 - 30703.8\varepsilon + 289440.2\varepsilon^2$
	540	$-\partial\ln\theta/\partial\varepsilon = 463.8 - 13541.2\varepsilon + 131183.9\varepsilon^2$
	560	$-\partial\ln\theta/\partial\varepsilon = 547.6 - 9668.3\varepsilon + 130935.5\varepsilon^2$
1	460	$-\partial\ln\theta/\partial\varepsilon = 349.2 - 105492.6\varepsilon + 713130.2\varepsilon^2$
	500	$-\partial\ln\theta/\partial\varepsilon = 286.4 - 36536\varepsilon + 451408.2\varepsilon^2$
	540	$-\partial\ln\theta/\partial\varepsilon = 527 - 26554.9\varepsilon + 232095\varepsilon^2$
	560	$-\partial\ln\theta/\partial\varepsilon = 208.9 - 9311.04\varepsilon + 129492.7\varepsilon^2$
10	460	$-\partial\ln\theta/\partial\varepsilon = 19320 - 611406\varepsilon + 3417790\varepsilon^2$
	500	$-\partial\ln\theta/\partial\varepsilon = 6043 - 235446\varepsilon + 1622740\varepsilon^2$
	540	$-\partial\ln\theta/\partial\varepsilon = 7982 - 185460.5\varepsilon + 1609900\varepsilon^2$
	560	$-\partial\ln\theta/\partial\varepsilon = 10615 - 209476.1\varepsilon + 2597670\varepsilon^2$

According to the two order fitting polynomial, at the point where $-\partial\ln\theta/\partial\varepsilon$ is the minimum

value, the corresponding strain is critical ε_c of dynamic recrystallization.

Peak strain ε_p is obtained from the true stress-strain curves. Critical strain ε_c and peak strain ε_p can be the function of Zenner-Hollomon parameter *Z* as shown in figure 8.

$$\varepsilon_p = 1.2 \times 10^{-2} Z^{0.069} \tag{9}$$

$$\varepsilon_c = 7.5 \times 10^{-3} Z^{0.073} \tag{10}$$

$$\varepsilon_c/\varepsilon_p \approx (0.678\sim0.707) \tag{11}$$

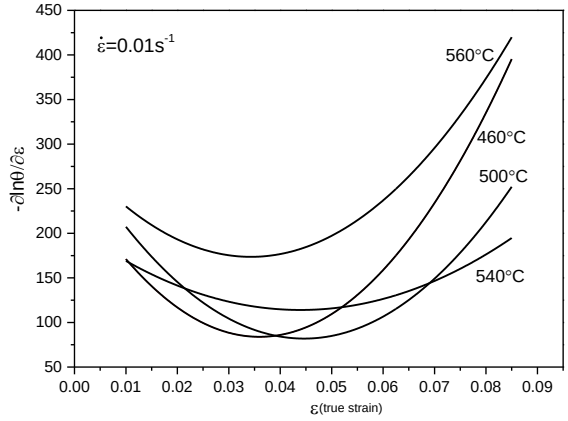

Figure 7. The $(-\partial \ln\theta/\partial\varepsilon) - \varepsilon$ curves of 6082 aluminum alloy at strain rate 0.01 s^{-1}.

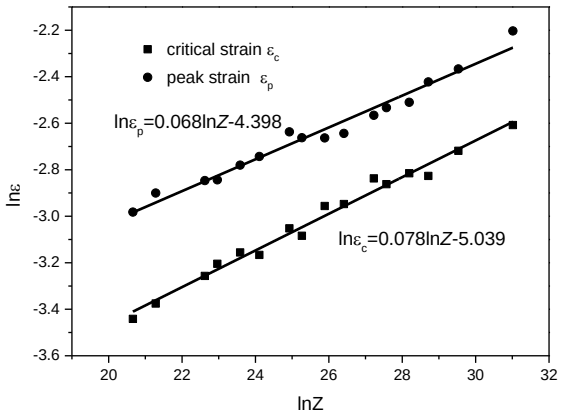

Figure 8. lnε_p versus ln*Z* and lnε_c versus ln*Z* plot.

4. Conclusions

The dynamic recrystallization behavior of 6082 Al-Si-Mg aluminum alloy is investigated by compression experiment in high temperature. The main results can be summarized as follows:

- At lower strain rates, hardening and softening due to dynamic recrystallization are in balance; at high strain rates, hardening and softening due to dynamic recrystallization alternately dominated.
- The deformation activation energy of 6082 Al-Si-Mg is about 174.9 kJ mol^{-1}.
- Lower strain rates are beneficial to increase the volume fraction of DRX, the average grain size is coarse; High strain rates are beneficial to refine average grain size, the volume fraction of DRX is less than that in low strain rates. High temperature cause coarse grains.
- The relationship between initial critical strain ε_c of dynamic recrystallization and Zenner-Hollomon parameter *Z*: ε_c=7.5×10^{-3}*Z* $^{0.073}$.
- $\varepsilon_c/\varepsilon_p \approx (0.678\sim0.707)$.

References

[1] Ebrahimi G R, Keshmiri, Maldar A R and Momeni A 2012 *Mater. Sci. Technol* **28** 467-73
[2] Liang T, Anderson I, Riedemann T and Russell A 2014 *Acta Materialia* **77** 151-61
[3] Poliak E I and Jonas J J 1996 *Acta Mater* **44** 127-36
[4] Liang T, Anderson I, Riedemann T and Russell A 2017 *Mater. Sci. Eng. A* **690** 348-54
[5] Liang T, Anderson I and Russell A 2017 *Materials Science* **49** 2787-94
[6] Luton M J and Sellars C M 1969 *Acta metal* **17** 1033
[7] Sellars C M 1981 *Metals Forum* **4** 75
[8] Poliak E I and Jonas J J 2003 *ISIJ International* **43** 684-91
[9] Guo H L, Sun Z C and Yang H 2013 *The Chinese Journal of Nonferrous Metals* **6** 1507-14
[10] Chen X H, Chen K H and Yang P X 2013 *The Chinese Journal of Nonferrous Metals* **1** 44-50

[11] Shi L, Yang H and Guo G 2014 *Journal of Plasticity Engineering* **1** 65-70
[12] Feng D, Zhang X M and Liu S D and Deng Y L 2014 *Mater. Sci. Eng. A* **608** 63-72
[13] Mirzadeh H and Najafizadeh A 2010 *Materials and Design* **31** 1174-9
[14] Zenner C and Hollmon J H 1944 *Journal of Applied Physics* **22** 22-32
[15] Peng J, Wang J Y and Zhong L P 2016 *Trans. Nonferrous Met. Soc. China* **26** 945-55